Multiobjective Generation and Transmission Expansion Planning of Renewable Dominated Power Systems using Stochastic Normalized Normal Constraint

Hamidreza Arasteh[a], Mohsen Kia[b], Vahid Vahidinasab[c], Miadreza Shafie-khah[d], João P. S. Catalão[e,1]

[a] *Power System Planning and Operation Group, Niroo Research Institute (NRI), Tehran, Iran*
[b] *Department of Electrical Engineering, Pardis Branch, Islamic Azad University, Pardis, Iran*
[c] *School of Engineering, Newcastle University, Newcastle upon Tyne, UK*
[d] *School of Technology and Innovations, University of Vaasa, 65200 Vaasa, Finland*
[e] *Faculty of Engineering of University of Porto and INESC TEC, Porto, Portugal*

Abstract

This paper proposes a comprehensive framework for generation and transmission planning of renewable dominated power systems, which is formulated as a stochastic multiobjective problem. In this regard, a Normalized Normal Constraint (NNC) solution approach is proposed to solve the introduced stochastic multiobjective generation and transmission planning (GTP) problem. The NNC is utilized in this paper as a relation between different objective functions with different dimensions to find the optimal weighting factors of these objectives. The NNC is applied for solving the GTP problem with objective functions including the investment and operation costs along with the transmission losses, while considering the cost of unserved energy, as well as the uncertainty of load and Renewable Energy Resources (RERs). A fuzzy-based decision making framework is utilized to select the best solution among the optimal non-dominated solution points. A scenario-based approach is used to model the uncertainties. The Garver 6-bus and IEEE 118-bus test systems are utilized to perform the numerical analysis. The simulation results validate the performance and importance of the proposed model, as well as the effectiveness of the NNC to find the evenly distributed Pareto solutions of the multiobjective problems.

Keywords: Generation and Transmission Expansion Planning; Renewable Power Systems; Stochastic Optimization; Multiobjective Problems.

Nomenclature

Indicators:

b: number of biomass units;
g: number of thermal units (coal, nuclear and combined cycle);
l: number of transmission lines;
lp: number of load points;
s: number of Concentrated Solar Power (CSP) units;
sc: number of scenarios;
w: number of wind turbines (offshore and onshore);
h: index of the horizon year;

[1] Corresponding author. E-mail address: catalao@fe.up.pt

Parameters:

$c^{g,I}$: per MW annualized installation cost of "g^{th}" thermal unit [$/MW];

$c^{w,I}$: per MW annualized installation cost of "w^{th}" wind turbine [$/MW];

$c^{s,I}$: per MW annualized installation cost of "s^{th}" CSP unit [$/MW];

$c^{b,I}$: per MW annualized installation cost of "b^{th}" biomass unit [$/MW];

c^{l} : annualized installation cost of "l^{th}" transmission line [$];

τ : rate of return;

h_{sc} : number of hours comprising scenario "sc";

$c^{g,O}$: per MWh operation cost of "g^{th}" thermal unit [$/MWh];

$c^{w,O}$: per MWh operation cost of "w^{th}" wind turbine [$/MWh];

$c^{s,O}$: per MWh operation cost of "s^{th}" CSP unit [$/MWh];

$c^{b,O}$: per MWh operation cost of "b^{th}" biomass unit [$/MWh];

$c^{lp,us}$: per MWh cost of unserved energy at point "lp" [$/MWh];

G^{l} : conductance of line "l" [℧];

h: horizon year;

N^{g}: total number of thermal units;

N^{w}: total number of wind turbines;

N^{s}: total number of CSP units;

N^{b}: total number of biomass units;

N^{l}: total number of transmission lines;

N^{lp}: total number of load points;

N^{sc}: total number of scenarios;

$N^{*}(lp)$: number of element * at point "lp";

$P_{sc}^{w,N}$: normalized generation of "w^{th}" wind turbine in scenario "sc" [p.u.];

$P_{sc}^{b,N}$: normalized generation of "b^{th}" biomass unit in scenario "sc" [p.u.];

$P^{g,I,max}$: maximum installable capacity of "g^{th}" thermal unit [MW];

$P^{w,I,max}$: maximum installable capacity of "w^{th}" wind turbine [MW];

$P^{s,I,max}$: maximum installable capacity of "s^{th}" CSP unit [MW];

$P^{b,I,max}$: maximum installable capacity of "b^{th}" biomass unit [MW];

$P_{sc}^{lp,N}$: normalized value of load "lp" in scenario "sc" [p.u.];

P^{lp} : average amount of load "lp" [MW];

P_{sc}^{lp} : total amount of load "lp" in scenario "sc" [MW];

$p^{l,max}$: maximum permissible flow of line "l" [MW];

X^{l} : reactance of line "l" [Ω];

ϕ^{z} : loads' demand factor at zone "z";

μ : percentage of the penetration level of the renewable energy resources;

Variables:

$C^{g,I}$: total installation cost of thermal units [$];

$C^{W,I}$: total installation cost of wind turbines [$];

$C^{S,I}$: total installation cost of CSP units [$];

$C^{B,I}$: total installation cost of biomass units [$];

$C^{L,I}$: total investment cost of transmission lines [$];

$C_{sc}^{G,O}$: total operation cost of thermal units in scenario "*sc*" [$];

$C_{sc}^{W,O}$: total operation cost of wind turbines in scenario "*sc*" [$];

$C_{sc}^{S,O}$: total operation cost of CSP units in scenario "*sc*" [$];

$C_{sc}^{B,O}$: total operation cost of biomass units in scenario "*sc*" [$];

C_{sc}^{UE} : total cost of unserved load in scenario "*sc*" [$];

f^{C} : total cost [$];

f_{sc}^{Loss} : amount of energy losses in scenario "*sc*" [MWh];

$p^{g,I}$: installed capacity of thermal units [MW];

$p^{w,I}$: installed capacity of wind turbines [MW];

$p^{s,I}$: installed capacity of CSP units [MW];

$p^{b,I}$: installed capacity of biomass units [MW];

γ^{l} : a binary variable (that is 1 if line "*l*" has been installed; and 0 if line "*l*" has not been installed);

$p_{sc}^{g,O}$: generating power of thermal units in scenario number "*sc*" [MW];

$p_{sc}^{w,O}$: generating power of wind turbines in scenario number "*sc*" [MW];

$p_{sc}^{s,O}$: generating power of CSP units in scenario number "*sc*" [MW];

$p_{sc}^{b,O}$: generating power of biomass units in scenario number "*sc*" [MW];

$p_{sc}^{lp,UE}$: amount of unserved load at point "*lp*" in scenario number "*sc*";

p_{sc}^{l} : transmitted flow of line "*l*" in scenario "*sc*" [MW];

$p_{sc}^{lp,SE}$: amount of served load at point "*lp*" in scenario number "*sc*" [MW];

$\delta_{sc}^{l,sen}$: phase angle of the sending end of transmission line "*l*";

$\delta_{sc}^{l,rec}$: phase angle of the receiving end of transmission line "*l*".

1. Introduction

The utilization of green power plants is highly interested in recent years, due to environmental issues in the future power systems. Since the capacity of Renewable Energy Resources (RERs) can exceed the demand of energy, these energy resources are considered to have an important share of the future energy portfolio. Moreover, the increasing environmental problems are other important reasons that motivate the relevant organizations to investigate the potential of clean energy resources [1]. Furthermore, RERs can optimally be used to reduce the losses of the transmission systems.

In 2008, the "climate and energy package" dealt with the European Union (EU) with the aim of reducing energy demand and cope with the climate change influences. The main goals of this package (that is named as "20-20-20 targets") could be classified as the follows [2].

- achieve twenty percent emission reduction in the EU, in comparison with the 1990's greenhouse emissions level;
- enhance the EU power production by using RERs, up to twenty percent;
- enhance the EU's energy efficiency, up to twenty percent.

In addition, US plans to enhance the penetration of RERs by ninety percent until 2050 [3].

Several studies have investigated the presence of RERs in the system [4-9]. Wu et al. [10] presented a control strategy based on reactive power regulation of DFIG-based wind farm. Hamidpour et al. [11] have studied the wind integrated power systems by considering the presence of demand response resources. Aghaei et al. [12] introduced a probabilistic mixed-integer linear programming (MILP) model by considering the plants and transmission lines contingencies. Pozo et al. [13] proposed an expansion model by considering the uncertainties of the wind turbines and hydro units, as well as electricity demand level. An MILP model has been presented in [14] to determine the optimal structure with the aim of designing a renewable dominated network. Ref. [15] reviews the recent activities regarding the integration of the RERs into the future smart grids. In [16], a multiobjective optimization problem is proposed to minimize the energy losses, voltage fluctuations, and cost terms, where the decision variable are to find the optimal size and location of the RERs and Electric Vehicle (EV) charging stations. Telukunta et al. [17] reviewed the protection schemas of a system with RERs and identified the merits and demerits of these methods. Ref. [18] provided an overview on the RER in Iran and their potentials. Liu et al [19] quantifies the techno-economic indicators (i.e. electricity production, costs and incomes, as well as emissions), through simulating the employment of RERs (including wind turbines, biomass units and solar cells). Ref. [20] studied the increasing energy demand in the Middle East and evaluated the potentials of RERs. Zwaan [21] estimated the potentials regarding renewable energy jobs in the Middle East. Mostafaeipour et al. [22] demonstrated the potentials of different RERs in the Middle East and Iran. Rourke et al. [23] investigated the potentials of RERs and the corresponding technologies in Ireland.

RERs have been focused not only on reducing the emission rate, but also on providing some other goals such as facilitating the energy access (especially in rural regions); enhancing the security level (with the diversification of the energy and technology portfolios); as well as progressing socially and economically (through potential employment opportunities) [1, 24]. Moreover, the RERs could be allocated optimally to provide other benefits such as loss reduction. In addition to reduce the dependency on fossil fuel-based resources, renewable resources can pave the road toward integration of more electric vehicles by providing charging power locally [25]. In [26], the SWOT (Strengths, Weaknesses, Opportunities, and Threats) analyses are utilized to determine the key factors which could affect the renewable energy technologies in Sindh and Baluchistan province. Several strategies have been described in this paper, such as:

- ✓ Introducing suitable policy plans and packages for establishing renewable power plants;
- ✓ Incentivize the stakeholders;
- ✓ Enhance the awareness and knowledge about the RERs;
- ✓ Establishing an entrepreneurship system in order to develop the renewable technologies.

In [27], a multi-agent based framework is proposed to optimize the operation of power distribution networks by leveraging the intermittencies of distributed energy resources and demand side management methods. Ref. [28] has assessed the climate change influences on wind power potentials in Brazil. The findings of this paper show that the wind power potentials may not be faced with high reductions in Brazil. Viviescas et al. [29] have evaluated the renewable energy contribution to energy security in Latin America. The investigation results from analyzing monthly and hourly correlations show that Brazil could have a pivotal role for integrating the RERs in Latin America. In fact, the statistical investigations revealed that Brazilian hotspots showed the highest potential for complementing and for being complemented by different Latin America countries. In addition, Venezuela shows strong correlations with countries such as Paraguay, Brazil and Ecuador, mainly under a seasonal pattern.

Different methods (i.e. multiobjective particle swarm optimization, non-dominated sorting genetic algorithm, weighting method, differential evolution method, epsilon constraint method, and normal boundary intersection) have been introduced to solve the multiobjective problems [9, 30-33]. Generally, the results of the multiobjective problems are a set of solutions that named as Pareto solutions/Pareto curve. One of the important features of the optimization method is that it should be able to search all the decision space. There are several methods to optimize the multiobjective problems, such as Weighted Sum (WS), goal attainment, Normal Boundary Intersection (NBI), multiobjective indirect optimization, multiobjective evolutionary algorithm, etc. [34]. Monsef et al. [35] have investigated the performance of the Non-Dominated Sorting Genetic Algorithm-II (NSGA-II), multiobjective differential evolution, and multiobjective particle swarm optimization by employing different mathematical test functions and four water distribution network (WDN) design under the same conditions. Costa et al. [36] have shown that the NBI approach is independent of the relative scales of the functions and could find the evenly distributed Pareto solutions [36]. The NBI algorithm is employed in [37] for co-optimizing three competing objective functions. The well effectiveness of the NBI is proved in this paper by comparing the results with two other methods, i.e. Scalar Optimization (SO) and NSGA-II. The performance of the NBI to optimize the multiobjective problems and find better Pareto solutions (considering the cost and emission, as well as solution time) is justified through the numerical results. NBI method is able to overcome the deficiencies of the WS (e.g., inability to find the evenly distributed Pareto points), especially when the multiobjective problem is non-convex. Unlike the WS approach, the NBI is able to find a near-uniform spread of Pareto solution points [38]. Ref. [39] showed that the NBI could trace nonconvex surfaces. Shukla et al. [40] performed a comparative study that have justified the better performance of the NBI compared to the WS to find the uniformly distributed Pareto solutions. The NNC is an approach that is proposed to solve the multiobjective problems and is able to generate evenly distributed solution points [41]. Rahmani et al. [42] presented an improved version of NNC to solve the multiobjective optimal power flow. Both the NBI and NNC methods are able to generate an evenly distributed Pareto solution points in an n-dimensional design space, be it convex or not. Compared to the NBI, the NNC approach has some important advantages, e.g., it is more computationally stable, and is less likely to find non-Pareto solution points [43]. Moreover, when the Pareto curve is obtained, the problem decision maker should select one of the solutions. Fuzzy set, analytical hierarchy process, knee set, and max–min methods are some of the algorithms to choose the final solution [30, 44]. However, the decision maker is able to select one of the solutions based on its priorities, privileges or existing limitations. Fuzzy sets are popular approaches to select the final solution point based on membership functions [45, 46]. The membership functions have the values in the range of 0-1, in which 0 represents incompatibility with the sets, while 1 indicates the full compatibility [45, 46]. The amount of this function will show that, how an objective function has been satisfied with a non-dominated Pareto solution. The sum of the membership functions for all the objective functions should be calculated to compute the “accomplishment” of the solutions in satisfying the objective functions. By normalizing the accomplishment of each non-dominated solution point over the sum of the accomplishments of all the non-dominated results, the accomplishments could be rated with respect to each other [47]. The solution with the maximum membership will be selected as the best solution (that has the highest priority ranking) [45].

The literature review and analyses show that in addition to the high need and interest to investigate the penetration of RERs and their impacts (different aspects such as economic planning and operation, energy losses, etc.), there is a high need to employ the efficient optimization algorithms, especially in the multiobjective problems. Therefore, the paper deals not only with different penetration level of RERs, as well as their technical and economic impacts, but also with the multiobjective optimization framework (that should be able to find an evenly distributed Pareto front). Indeed, this paper aims to propose a model to lead the conventional power systems towards the fully RER-based systems. The planning of generation and transmission systems is considered in this paper. The problem is a multiobjective optimization to minimize both the planning costs and the power losses. From this point of view, the effects of different penetration levels of the RERs on the planning and operation costs, as well as their impacts on the total energy losses are analyzed, in order to determine the optimal penetration level from both the economic and technical aspects. The uncertainties of the demand level, solar and wind generations are modeled by using the K-means technique. The NNC method is proposed to solve the introduced multiobjective problem. The main advantage of this method is its ability to evenly search all the decision space and scape from some sub-optimal solutions.

Briefly, compared to the existing studies, the main contributions of this paper are to:

1) a multiobjective framework is proposed for the planning and operation of the composite generation and transmission systems;
2) the NNC method is developed for the planning and operation of the renewable-dominated power systems to find an evenly distributed Pareto curve; and
3) the optimal planning and operation strategies are decided based on the fuzzy-based decision making framework.

The rest of the paper is organized as follows. The problem descriptions (the formulation of the objective functions and constraints, as well as the method used in this paper to model the uncertain parameters) are described in section 2. The NNC procedure to solve the multiobjective problems is introduced in section 3. Section 4 is devoted to the simulation results and analysis. Finally, concluding remarks are drawn in section 5.

2. Problem description

As mentioned, the planning and operation of the integrated generation and transmission systems by considering the cost terms, as well as energy losses as the objective functions is discussed in this paper. Although these terms could be modeled with a single-objective problem, the multiobjective model is considered here to enhance the accuracy of the proposed model.

The mathematical definitions of the different terms of the objective functions, and the relevant constraints of the problem, as well as the scenario generation procedure are described in this section.

2.1. Objective functions

The first objective function is to minimize the total investment and operation costs that is comprised of the following terms:

The installation cost of thermal units: Total cost to install the thermal units that could be formulated as (1).

$$C^{g,I} = \sum_{g=1}^{N^g} c^{g,I} p^{g,I} \tag{1}$$

The installation cost of wind turbines: Total cost to install the wind turbines that is computed by (2).

$$C^{W,I} = \sum_{w=1}^{N^w} c^{w,I} p^{w,I} \tag{2}$$

The installation cost of concentrated solar power (CSP) units: The required cost to install the Concentrated Solar Power (CSP) units that is presented as (3).

$$C^{S,I} = \sum_{s=1}^{N^s} c^{s,I} p^{s,I} \tag{3}$$

The installation cost of biomass units: Total cost to install the biomass units as formulated by (4).

$$C^{B,I} = \sum_{b=1}^{N^b} c^{b,I} p^{b,I} \tag{4}$$

The installation cost of transmission lines: The required cost to install transmission lines (5).

$$C^{L,I} = \sum_{l=1}^{N^l} c^l \gamma^l \tag{5}$$

It should be noted that the capital recovery factor (CRF) is used to annualize the installation cost terms, as formulated by (6).

$$CRF = \frac{\tau(1+\tau)^h}{(1+\tau)^h - 1} \tag{6}$$

The operation cost of thermal units: Equation (7) formulates the operation cost of thermal units.

$$C_{sc}^{G,O} = h_{sc} \sum_{g=1}^{N^g} \left(c^{g,O} p_{sc}^{g,O} \right), \ \forall sc \tag{7}$$

The operation cost of wind turbines: The operation cost of wind turbines is expressed by (8).

$$C_{sc}^{W,O} = h_{sc} \sum_{w=1}^{N^w} \left(c^{w,O} p_{sc}^{w,O} \right), \ \forall sc \tag{8}$$

The operation cost of CSP units: The operation cost of CSP units could be computed by (9).

$$C_{sc}^{S,O} = h_{sc} \sum_{s=1}^{N^s} \left(c^{s,O} p_{sc}^{s,O} \right), \ \forall sc \tag{9}$$

The operation cost of biomass units: Equation (10) defines the operation cost of biomass units.

$$C_{sc}^{B,O} = h_{sc} \sum_{b=1}^{N^b} \left(c^{b,O} p_{sc}^{b,O} \right), \ \forall sc \tag{10}$$

The cost of unserved energy: The cost term that is relevant to the unserved energy could be calculated by (11).

$$C_{sc}^{UE} = h_{sc} \sum_{lp=1}^{N^{lp}} \left(c^{lp,us} p_{sc}^{lp,UE} \right), \ \forall sc \tag{11}$$

Therefore, the first objective function can be formulated as (12).

$$\begin{aligned} f^C = & CRF \left[C^{G,I} + C^{W,I} + C^{S,I} + C^{B,I} + C^{L,I} \right] \\ & + \sum_{sc=1}^{N^{sc}} \left(C_{sc}^{G,O} + C_{sc}^{W,O} + C_{sc}^{S,O} + C_{sc}^{B,O} + C_{sc}^{UE} \right) \end{aligned} \tag{12}$$

The second objective function is to minimize the total energy losses. As it is proved in [48], the total energy losses could be approximately formulated by equation (13).

$$f^{Loss} = \sum_{sc=1}^{N^{sc}} \left(h_{sc} \sum_{l=1}^{N^l} G^l \left(X^l p_{sc}^l \right)^2 \right) \tag{13}$$

The linearization of this equation has been presented in [2].

2.2. Constraints

Power balance: Total power generation and consumption should be equal with each other.

$$\sum_{g=1}^{N^g(lp)} p_{sc}^{g,O} + \sum_{w=1}^{N^w(lp)} p_{sc}^{w,O} + \sum_{s=1}^{N^s(lp)} p_{sc}^{s,O} + \sum_{b=1}^{N^b(lp)} p_{sc}^{b,O} - p_{sc}^{lp,SE} = \sum_{l=1}^{N^l(lp)} p_{sc}^{l}, \quad \forall \ sc, \ lp \tag{14}$$

Maximum generation limits: This set of constraints indicate the permissible generation of each unit.

$$0 \le p_{sc}^{g,O} \le p^{g,I}, \ \forall \ sc, g \tag{15}$$

$$0 \le p_{sc}^{w,O} \le P_{sc}^{w,N} \times p^{w,I}, \ \forall \ sc, w \tag{16}$$

$$0 \le p_{sc}^{s,O} \le p^{s,I}, \ \forall \ sc, s \tag{17}$$

$$0 \le p_{sc}^{b,O} \le P_{sc}^{b,N} \times p^{b,I}, \ \forall \ sc, b \tag{18}$$

Maximum installation limits: The maximum values of the investments could be formulated by the following equations.

$$p^{g,I} \le P^{g,I,max}, \ \forall \ g \tag{19}$$

$$p^{w,I} \le P^{w,I,max}, \ \forall \ w \tag{20}$$

$$p^{s,I} \le P^{s,I,max}, \ \forall \ s \tag{21}$$

$$p^{b,I} \le P^{b,I,max}, \ \forall \ b \tag{22}$$

Supplied and un-supplied demands: The amounts of served and unserved energies are calculated as the following.

$$P_{sc}^{lp} = \phi^z P_{sc}^{lp,N} P^{lp} = p_{sc}^{lp,SE} + p_{sc}^{lp,UE}, \ \forall \ sc, \ lp \tag{23}$$

$$0 \le p_{lp,sc}^{UE} \le p_{sc}^{lp}, \ \forall \ sc, \ \forall \ lp \tag{24}$$

Power flow: The power flow calculations are handled by using the following equations.

$$p_{sc}^{l} = \frac{1}{X^l}\left(\delta_{sc}^{l,sen} - \delta_{sc}^{l,rec}\right), \ \forall \ sc, \ l \tag{25}$$

$$-p^{l,max} \le p_{sc}^{l} \le p^{l,max}, \ \forall \ sc, \ l \tag{26}$$

Maximum penetration of RESs: The penetration of the RESs may be restricted as presented by (27).

$$p^{w,I} + p^{s,I} + p^{b,I} \le \mu\left(p^{g,I} + p^{w,I} + p^{s,I} + p^{b,I}\right) \tag{27}$$

It should be mentioned that for the sake of simplicity and loss of generality, other components (such as storage units), as well as some constraints (such as ramping constraints) are not considered here.

2.3. Scenario generation

In the power system studies, there are some parameters that are based on the forecast values [49] and therefore are uncertain. As mentioned in [2], considering these uncertainties as the independent parameters could be resulted in the suboptimal decisions. Therefore, in the power systems, it could be beneficial to consider the statistical correlation between the uncertain parameters on the basis of the loads' historical data. The introduced procedure in [2] is used in this paper for generating the scenarios, in which, a single scenario could be constituted from the historical data of a day that comprises the amount of the load level, as well as the solar and wind generations in different locations. Then, a clustering method is used to reduce the scenario set to a tractable data set for grouping data based on the similarities. In this paper, the K-means technique is employed for clustering, in which the uncertain parameters are the load levels, as well as the solar and wind power generation. This method is based upon the selection of few points as the center of the clusters, and the assessment of the points to the closest cluster (according to the shortest path between the points and the centers of the clusters). The details of this method are explained in [2, 50].

3. The proposed NNC framework

To introduce the performance of the NNC method, (28) is considered as a common multiobjective problem.

$$\begin{aligned} &Min \ \ \{F_k\}, \ \ 1 \le k \le K \\ &S.T. \\ &\vartheta_i(x) \le 0, \ \ 1 \le i \le I \\ &\varsigma_j(x) = 0, \ \ 1 \le j \le J \\ &x_e \ge 0, \qquad 1 \le e \le E \end{aligned} \tag{28}$$

where, F_k denotes the objective functions and $\vartheta_i(x)$ $\varsigma_j(x)$ denote the inequality and equality constraint functions of the problem, respectively. x denotes the decision variables of the problem. Besides, K, I, J and E are the number of objective functions, the number of inequality constraints, the number of equality constraints, and the constraints of the decision variable, respectively. Moreover, k, i, j and e are the relevant indicators.

The procedure of the NNC to optimize a multiobjective problem is introduced at the following by considering K=2 (a problem with two objective functions). Fig. 1 illustrates the flowchart of the NNC technique. Each step is described as the following.

a) Determination of the anchor points

The first step is to find the best solution points of each objective function (anchor points). Therefore, the problem should individually be solved with the aim of optimizing each objective function. Fig. 2 illustrates the decision space, as well as the anchor points. In this figure, F_1 and F_2 are the assumed objective functions, while F_1^{min}, F_1^{max}, F_2^{min} and F_2^{max} are the minimum and maximum values of them. It is assumed that, A is the best solution of the F_2, while B is the best solution of the F_1.

b) Normalization of the objective functions

The second step is to normalize the values of objective functions and evaluate the Utopia line vector. The mapping procedure should be done by using the (29).

$$\alpha = \left\{\bar{F}_1, \bar{F}_2\right\}^T = \left\{\frac{F_1 - F_1^{\min}}{F_1^{\max} - F_1^{\min}}, \frac{F_2 - F_2^{\min}}{F_2^{\max} - F_2^{\min}}\right\}^T \tag{29}$$

where, $\bar{F}$ is the normalized vector of the objective functions. The normalized solution values and a typical Pareto curve of the solutions are shown in Fig. 3. A* and B* are the normalized anchor points.

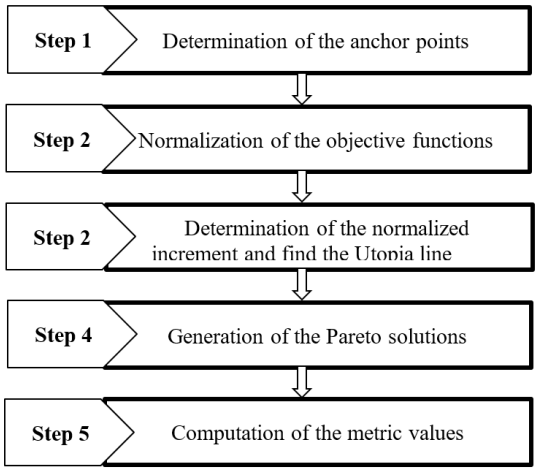

Fig. 1. The procedure of the NNC method

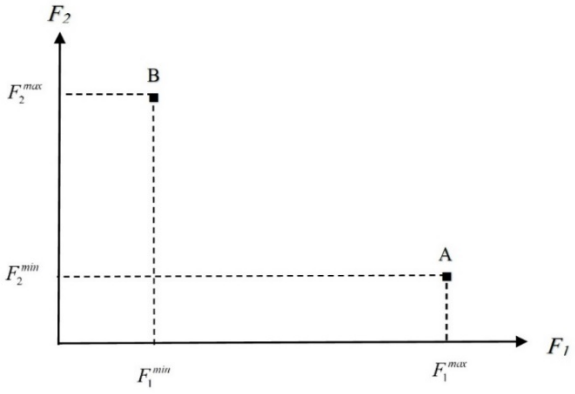

Fig. 2. The decision space, as well as the anchor points

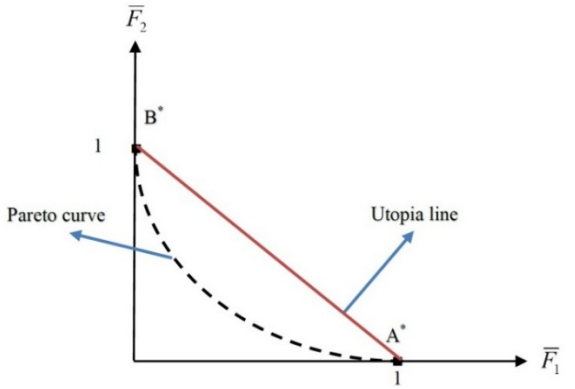

Fig. 3. The normalized solution values, as well as a typical Pareto curve of the solutions

Utopia line vector is defined as a vector to from B* to A* that is formulated by (30). This vector is also illustrated in Fig. 3.

$$U = A^* - B^* \tag{30}$$

In (30), U denotes the Utopia line vector.

c) Determination of the normalized increment and find the Utopia line points

Normalized increment should be determined to specify the solution intervals on the Pareto curve. If "s" is the number of desired solution points, the normalized increment (ξ) is calculated as (31).

$$\xi = \frac{1}{s-1} \tag{31}$$

Then, the Utopia line points (P_p) could be specified by using (32).

$$P_p = \eta_{1,p} B^* + \eta_{2,p} A^*, \quad p \in \{1, \ 2, \ ..., \ s\} \tag{32}$$

in which,

$$\begin{cases} 0 \le \eta_{1,p} \le 1 \\ 0 \le \eta_{2,p} \le 1 \\ \eta_{1,p} + \eta_{2,p} = 1 \end{cases}, \quad p \in \{1, \ 2, \ ..., \ s\} \tag{33}$$

It should be noted that, $\eta_{1,p}$ and $\eta_{2,p}$ are incremented by ξ between 0 and 1. The Utopia line points are shown in Fig. 4.

d) Generation of the Pareto solutions

The purpose of this step is to find the Pareto solutions of the multiobjective problem. Consider (28) as the main formulation of the problem. In this step, the problem is considered as (34). Equation (34) is a problem with one objective function, but new constraints are added to this new formulation. In this equation, k^* denotes one of the objective functions as the main objective of this new formulation (here, $k^*=2$). The new problem should be optimized frequently, where the new constraints should be updated in each run. The number of runs is equal to the number of Utopia line points. The performance of the new constraints is illustrated in Fig. 5. Indeed, the new constraints will omit some parts of the solution space in a way that in each run, the optimum solution point will find the best point within the new decision space. In Fig. 5, $\|U\|$ is the normal line of the Utopia point that limits the decision space to the new space (as it is shown on the figure).

According to Fig. 5, by considering the infeasible space that is removed from the old decision space (in the process of the NNC), if the problem is solved with the aim of optimizing F_2, the solution point C (that is shown in this figure) will be achieved as the best solution. By continuing this procedure, the Pareto curve solutions could be obtained that are well-distributed on all the decision space. Therefore, the NNC can guarantee that the optimization tool is able to search all the decision space.

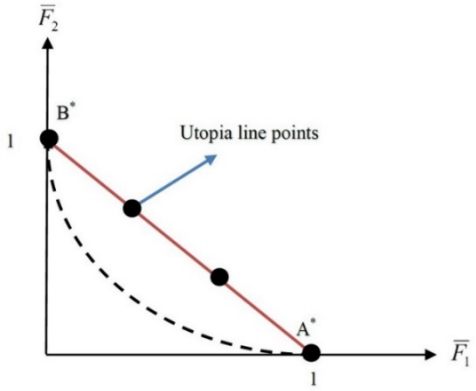

Fig. 4. The Utopia line points [41]

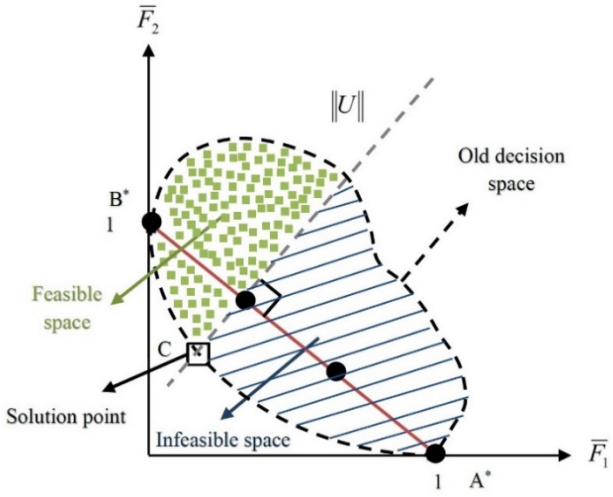

Fig. 5. The performance of the new constraints [41]

$$
\begin{aligned}
&Min\ \left\{F_{k^*}\right\}\\
&S.T.\\
&\vartheta_i(x)\le 0,\ \ 1\le i\le I\\
&\varsigma_j(x)=0,\ \ 1\le j\le J\\
&x_e\ge 0,\qquad 1\le e\le E\\
&U\left(\alpha-P_p\right)^T\le 0,\ \ p\in\{1,\ 2,\ ...,\ s\}\\
&\alpha=\left[\bar{F}_1\ \ \bar{F}_2\right]^T
\end{aligned}
\tag{34}
$$

e) Computation of the metric values

The last step is to compute the metric values. By using the obtained normalized values as the solutions of the problem, as well as the normalization procedure, the metric values could be computed.

Finally, it should be noted that, if the generated solutions are dominated by other points, they should be removed from the Pareto solutions.

4. Fuzzy-based decision-making tool

The fuzzy membership function is used here to select a specific solution among the Pareto curve. For this purpose, a linear membership function is employed for each of the objective functions as the following [51, 52]:

$$
\partial_r^y=\begin{cases}
1 & ,\quad f_r^y\le f_r^{min}\\
\dfrac{f_r^{max}-f_r^y}{f_r^{max}-f_r^{min}} & ,\quad f_r^{min}\le f_r^y\le f_r^{max}\ \ ,\ \ r=1,\ 2\\
0 & ,\quad f_r^y\ge f_r^{max}
\end{cases}
\tag{35}
$$

where, f_r^y is the "r^{th}" objective function in the "y^{th}" Pareto solution point, and ∂_r^y is its membership function. Furthermore, by considering the objective functions as the minimization problems, f_r^{min} is the satisfactory (minimum) amount of the "r^{th}" objective function, and f_r^{max} is its unsatisfactory value. The membership function of the "y^{th}" non-dominated solution could be normalized as (36) [51]:

$$
\partial^y=\frac{\sum_r\theta_r\partial_r^y}{\sum_{y=1}^{Y}\sum_r\theta_r\partial_r^y}
\tag{36}
$$

in which, θ_r and "Y" are the weight value of the "r^{th}" objective function, and the number of Pareto solution points, respectively. "θ_r" can be valued by the operator on the basis of its importance. The maximum amount of "∂^y" shows the most preferred compromise solution and can be selected as the final solution [51].

5. Numerical study

The Garver's six-bus, as well as the modified IEEE 118-bus test systems are utilized here for the sake of analyzing the simulation results [14, 53]. All the input data are extracted from [2]. As mentioned, K-means clustering method is used to reduce total generated scenarios (8760 demand-CSP-wind scenarios are generated and then reduced to 10 clusters). The samples of demand and CSP, as well as wind scenarios are depicted in Fig. 6 by blue points that are grouped in 10 clusters to represent 10 scenarios (black points).

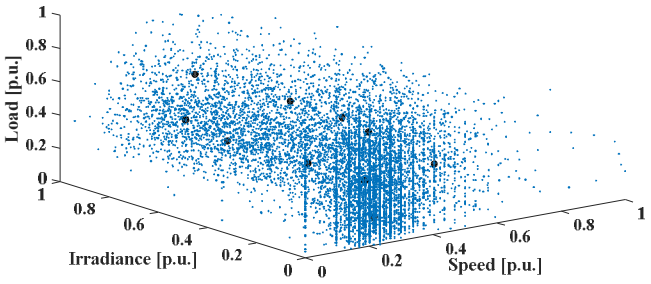

Fig 6. Samples of demand/CSP/wind scenarios clustering

The planning horizon is 20 years. The simulation analysis is done with five different rates of return: 5, 7, 9, 11 and 13 % (when the changes of the rate of return parameter are analyzing, the constraint (27) is relaxed). As pre-mentioned, the final solution is selected by the decision maker based on the fuzzy approach. A linear membership function is considered as introduces in [2].

5.1. Garver's six-bus system

For the ease of access, the cost terms of the units and the characteristics of the candidate lines are provided in Tables 1 and 2, respectively (it should be noted that, as mentioned in previous sections, thermal units include all the coal, nuclear and combined cycle units that are separately mentioned in this section). The Pareto solutions of the problem by using the NNC method for the Garver's six-bus system are shown in Fig. 7. In this figure, the Pareto curves are illustrated for different values of τ .

Figs. 8-a and 8-b illustrate the installed capacity of different units with respect to the various values of τ and μ. It should be noted that, although the total demand in this system is 760 MW, the installed capacity of the units is higher than the demand. This is because of the availability of the uncertain power resources. It is noteworthy that, if the value of the CRF is increased, then the optimization problem will select more dispatchable (non-renewable) units rather than non-dispatchable (renewable) resources.

Table 1

The cost terms of the Garver's six-bus system [2]

Type	Bus number	Installation cost [$/kW]	Fuel/emission/ operating/ maintenance cost [$/MWh]	Capacity [MW]
Nuclear	4	3610.9	11.37	500
Combined cycle (CC)	3	1218.7	46.95	250
Coal with CCS*	1	2955.7	26.93	230
Onshore wind	2	1756.3	4.87	150
Offshore wind	6	2843.6	7.69	300
Concentrated solar power	2	3287.0	1.87	200
Concentrated solar power	5	3288.3	1.69	150
Biomass	5	2133.9	38.20	200

* CCS: Carbon Capture and Storage

Table 2

The characteristics of the candidate lines of the Garver's six-bus system [2]

From-To	X [per-unit]	G [per-unit]	Capacity [MW]	Investment cost [×10^6$]
1-3	0.38	0.0129	100	51.70
1-6	0.68	0.0119	70	104.70
2-5	0.31	0.0132	100	18.60
2-6	0.30	0.0025	100	67.30
3-4	0.59	0.0209	82	16.19
3-6	0.48	0.0059	100	37.40
4-5	0.63	0.0187	75	26.50
4-6	0.30	0.0484	100	69.10
5-6	0.61	0.0086	78	78.05

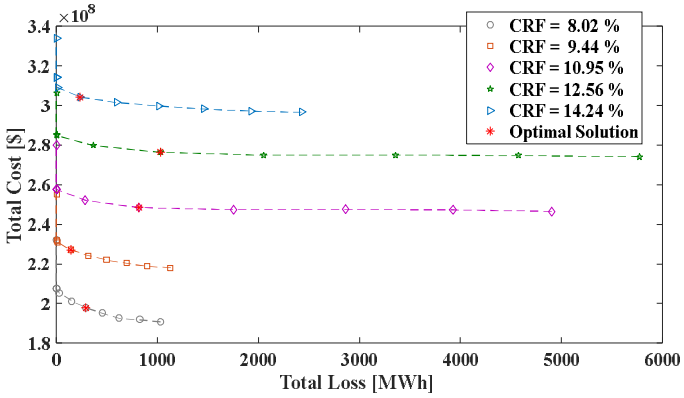

Fig. 7. The Pareto curve solutions of the Garver's six-bus system

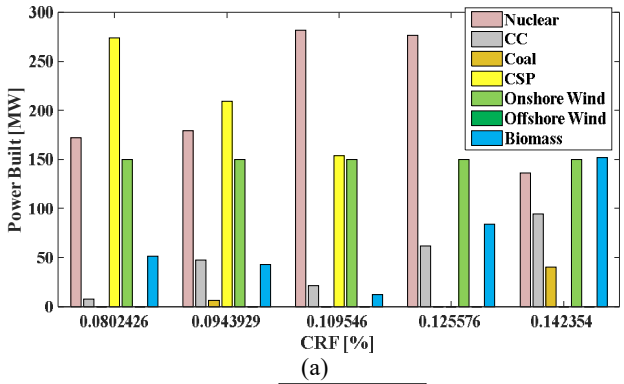

(a)

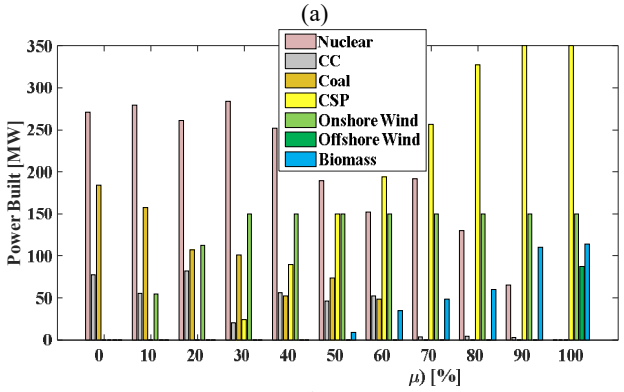

(b)

Fig. 8. The installed capacity of different units for the Garver's six-bus system: a) for different values of τ ; b) for different values of μ

By considering eleven different values for the μ (in the range of 0 to 100 percentage) and assuming the CRF to be 10 %, the utilization level of renewable resources (as it is shown in Fig. 8-b) will be enhanced. According to this figure, by increasing the value of μ, more capacities of renewable resources will be used. It could be observed that, when the penetration level of RERs is 0%, the capacity of installed RERs is 0. By increasing the permissible penetration level of the RERs, the installed capacity of these units is increasing. Finally, when the penetration rate of them is 100%, the capacity of these resources reaches to the maximum required power (and the capacity of installed thermal units is 0). As it is observed, the most preferred renewable resource is onshore wind turbines, while offshore wind turbines are the last preferred renewable units. Moreover, as it can be observed in these figures, due to the high investment cost of the CSP units, the installation of CSP units are dramatically growing-up when the penetration level of RERs is considered to be more than 30 %. It should be noted that, because of the high investment cost of CSP units, the capacity of these resources is near to zero, when the penetration level of the RERs is lower that 30%. However, these units have the minimum operation costs among other units. When the maximum permissible penetration of the RERs is increasing, their lower operational costs will dominate other cost terms. Therefore, the utilization of these units with lower operational cost will be more economical. Hence, when the maximum penetration level of the RERs is higher than 30%, the CSP units will play more important roles to satisfy the forecasted demand.

The energy losses of the 6-bus system are shown in Fig. 9. These results are evaluated for different values of μ and P_p (Utopia line points). As can be seen in Fig. 9, with increasing the penetration level of RERs, total energy losses are first reduced and then increased. The reason for such variations is that from the loss function point of view, the optimal penetration of RERs will be a value between its minimum and maximum possible values. The figure indicates when the objective is loss reduction, the optimal point of RER penetration does not happen in the highest penetration level. Indeed, if the optimization function is only to minimize the energy losses, the results for the penetration level of RERs will not necessarily be equal to their maximum values, but it could gain other penetration values (among the permissible range) depended to the specifications of the system under study.

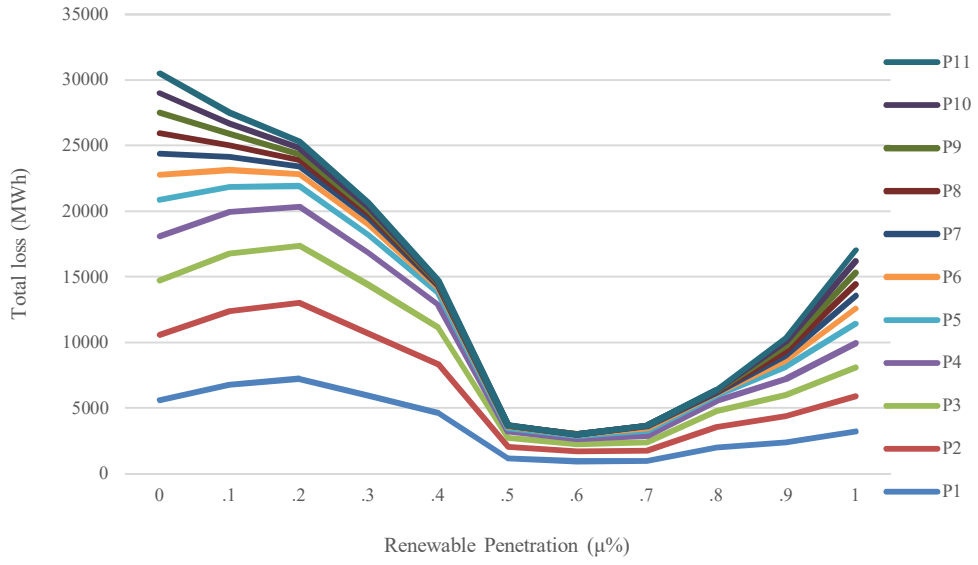

Fig. 9. Energy losses of the Garver's six-bus system for different values of μ and Pp

The installation and operation costs of thermal and renewable units, as well as the transmission lines are shown in Fig. 10-a and 10-b. These results are illustrated for different values of μ. According to Fig. 10, the investment cost of transmission lines is low compared to the installation costs of the generating units. Also, the installation costs of non-dispatchable resources are higher than the dispatchable units, while their operation costs are less than the thermal units.

According to Fig. 10-b, when the penetration level of RERs is around 70%, the total operation cost of thermal units is approximately equal to the total operation cost of RERs.

5.2. Modified IEEE 118-bus test system

In order to investigate the performance of the proposed problem and the validity of the results, all the results are also provided here for the modified IEEE 118-bus test system. Based on the IEEE 118-bus test system, three different zones could be considered for this system, as shown in Table 3.

The Pareto solutions of the problem by using the NNC method for the 118-bus test system is shown in Fig. 11. Different values of τ are considered and shown in this figure. Moreover, Figs. 12-a and 12-b illustrate the installed capacity of different units with respect to the various values of τ and μ. As an example, it can be seen in these figures that the installation of CSP units is increased rapidly when the penetration level of RERs is more than 40 % (due to the high installation cost of these units).

Fig. 13 shows the energy losses of the 118-bus test system for different values of μ and P_p. As previously observed, the amount of the energy losses is changing with the variation of the RERs penetration level.

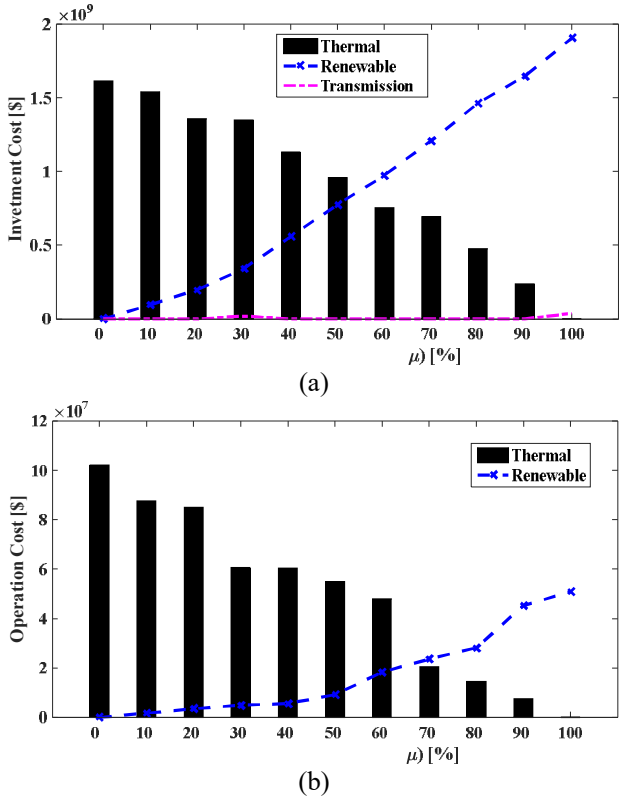

Fig. 10. The installation and operation costs of the Garver's six-bus system: a) installation costs; b) operation costs

Table 3

Different zones of the modified IEEE 118-bus system

Zone numbers	Buses	Demand factor
1	1–32, 113–115, 117	2.5
2	33–64	1.75
3	65–112, 116, 118	3.25

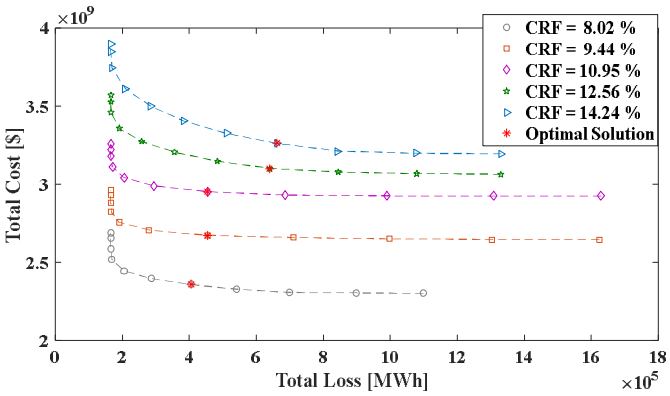

Fig. 11. The Pareto curve solutions of the 118-bus test system

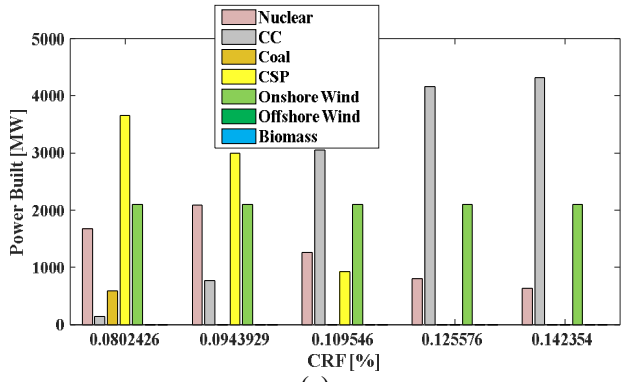

(a)

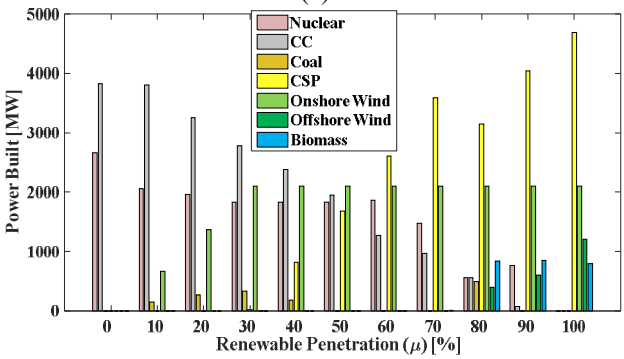

(b)

Fig. 12. The installed capacity of different units for the 118-bus test system: a) for different values of τ ; b) for different values of μ

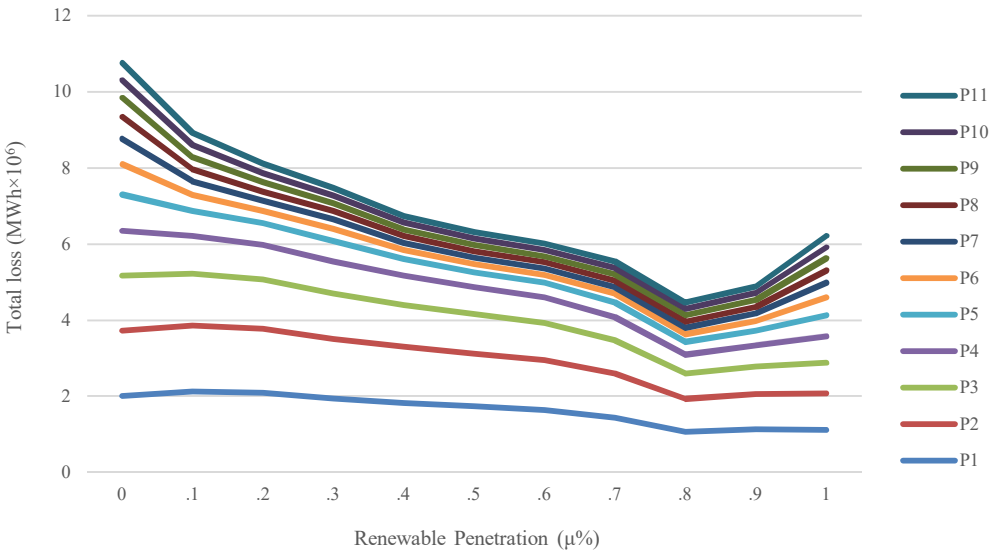

Fig. 13. Energy losses of the 118-bus test system for different values of μ and Pp

The installation and operation costs of thermal and renewable units, as well as the transmission lines are shown in Fig. 14-a and 14-b. These results are illustrated for different values of μ .

Finally, in order to show the performance of the NNC method to evenly search the decision space, the Pareto solutions of the proposed NNC method are compared with the NBI approach that is one of the best methods to solve the multiobjective problems. Fig. 15 illustrates the comparison results.

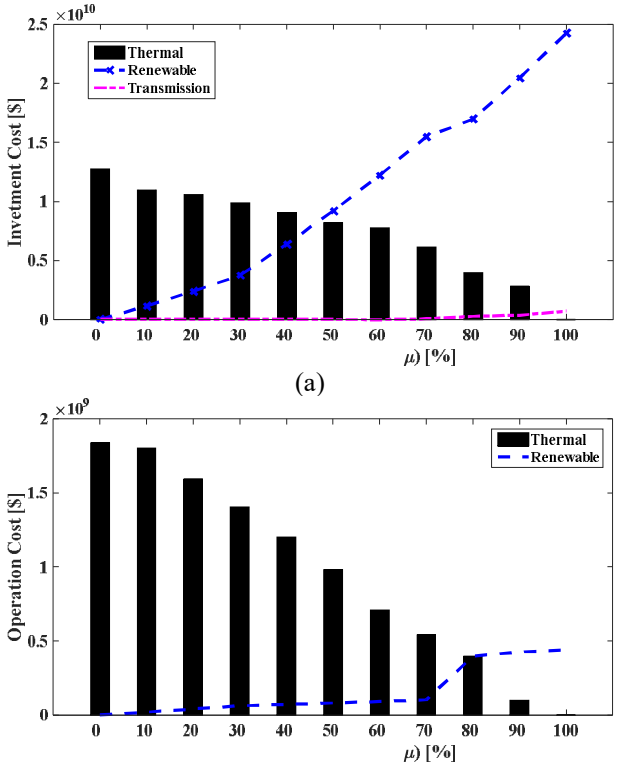

Fig. 14. The installation and operation costs of the 118-bus test system: a) installation costs; b) operation costs

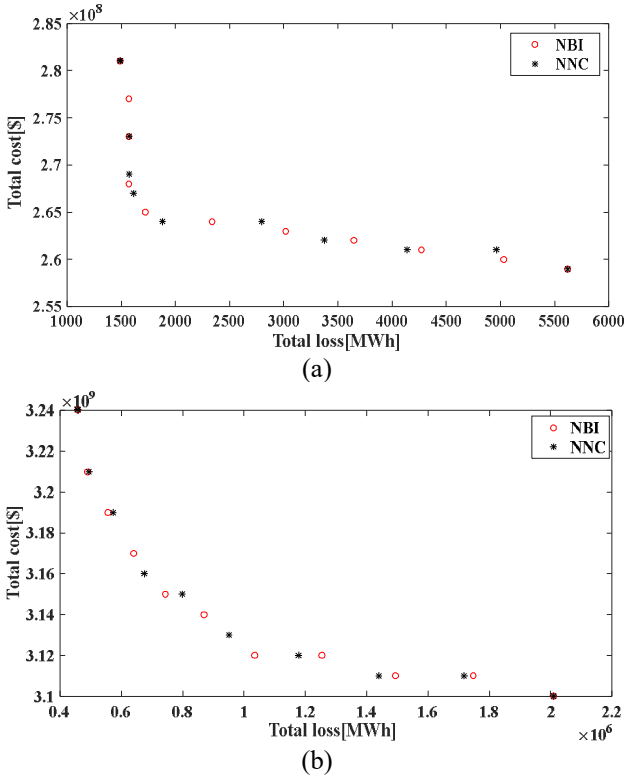

Fig. 15. The Pareto curve solutions of the NBI and NNC methods: a) Garver's six-bus system; b) 118-bus test system

As it could be observed in this figure, the NNC approach is able to effectively search all the decision space and the solution points are evenly distributed over the decision space.

6. Conclusions

The paper addressed the multiobjective planning and operation of the generation and transmission systems, in which the planning and operation costs, as well as the power losses of the system were considered as the objectives of the problem. Different penetration levels of RERs were analyzed to investigate the transformation of thermal-based systems towards the renewable-based ones. According to the results, by increasing the penetration level of RERs, total energy losses are first reduced and then increased. This shows that, if the objective function is only to minimize the energy losses, the best penetration level of RERs may be obtained at a point between the minimum and maximum permissible values. Moreover, the most and the last preferred renewable units are examined that are depended to the specifications of the system under study. In addition, it is illustrated that, on the basis of the installation and operation cost of different units, total penetration level of renewable resources may affect the optimal combination of different RERs (as an instance, for the Garver's six-bus system, when the penetration level of the RERs is lower that 30 %, the capacity of these resources is near to zero, while it is dramatically growing-up by increasing the total penetration of renewable resources to be more than 30 %. Similarly, for the introduced 118-bus test system, the installation of CSP units is increased rapidly when the penetration level of RERs is more than 40 %). The NNC method was utilized to solve the presented multiobjective problem. The fuzzy-based approach is employed in order to specify the final optimal solution point among the Pareto solutions. The investigation results showed that the optimal topology of the system was affected by both the objectives, i.e. the cost terms, as well as the power losses. Moreover, it was shown that the NNC technique is sufficient to obtain the evenly distributed Pareto solutions (that is an important feature of an optimization tool to be able to search all the decision space and scape from the local optimum points). The paper could be continued to consider more than two objectives as the main goals of the problem and to develop the optimization approach to be efficient to solve the problem with more than two objectives. Moreover, the future trends of the study are to investigate the penetration of the storage systems and evaluate the flexibility of the system with respect to the penetration level of RESs and storage systems.

Acknowledgment

The work of M. Shafie-khah was carried out in SolarX research project with financial support provided by the Business Finland, 2019-2021 (grant No. 6844/31/2018). J.P.S. Catalão acknowledges the support by FEDER funds through COMPETE 2020 and by Portuguese funds through FCT, under POCI-01-0145-FEDER-029803 (02/SAICT/2017).

References

[1] Ellabban, O., Abu-Rub, H., Blaabjerg, F. Renewable energy resources: Current status, future prospects and their enabling technology. Renew Sustain Energy Rev, 2014, 39, pp 748–764.

[2] Bagheri, A., Vahidinasab, V., Mehran, K. A novel multiobjective generation and transmission investment framework for implementing 100% renewable energy sources. IET Gener Transm Distrib, 2018, 12, 2, pp 455-465.

[3] Hand, M. Renewable electricity futures study. (National Renewable Energy Laboratory). 2012.

[4] Samal, RK. Tripathy, M. Cost savings and emission reduction capability of wind-integrated power systems. Int J Electr Power Energy Syst, 2019, 104, pp 549–561.

[5] Wang, S. Luo, F. Dong, ZY. Ranzi, G. Joint planning of active distribution networks considering renewable power uncertainty. Int J Electr Power Energy Syst, 2019, 110, pp 696-704.

[6] Misaghian, MS., Saffari, M., Kia, M., Heidari, A., Shafie-khah, M., Catalão, JPS. Tri-level optimization of industrial microgrids considering renewable energy sources, combined heat and power units, thermal and electrical storage systems. Energy, 2018, 161, pp 396-411.

[7] Bahrami, S., Amini, MH., Shafie-khah, M., Catalao, JPS. A decentralized renewable generation management and demand response in power distribution networks. IEEE Trans Sustain Energy, 2018, 9, 4, pp 1783-1797.

[8] Abdollahi-Mansoorkhani, H., Kia, M., Sahebi, MM. Stochastic security-constrained unit commitment with ARMA-based wind modelling considering network uncertainties. Int J Renew Energy Res, 2013, 3, 1, pp 132-137.

[9] Arasteh, H., Vahidinasab, V., Sepasian, MS., Aghaei, J. Stochastic system of systems architecture for adaptive expansion of smart distribution grids. IEEE Trans Ind Inf, 2019, 15, 1, pp 377 - 389.

[10] Wu, X., Guan, Y., Yang, X., Ning, W., Wang, M. Low-cost control strategy based on reactive power regulation of DFIG-based wind farm for SSO suppression. IET Renew Power Gener, 2019, 13, 1, pp 33–39.

[11] Hamidpour, H., Aghaei, J., Dehghan, S., Pirouzi, S., Niknam, T. Integrated resource expansion planning of wind integrated power systems considering demand response programs. IET Renew Power Gener, 2019, 13, 4, pp 519-529.

[12] Aghaei, J., Amjady, N., Baharvandi, A., Akbari, MA. Generation and transmission expansion planning: MILP-based probabilistic model. IEEE Trans Power Syst, 2014, 29, 4, pp 1592–1601.

[13] Pozo, D., Sauma, EE., Contreras, J. A three-level static MILP model for generation and transmission expansion planning. IEEE Trans Power Syst, 2013, 28, 1, pp 202–210.

[14] Dominguez, R., Conejo, AJ., Carrion, M. Toward fully renewable electric energy systems. IEEE Trans Power Syst, 2015, 30, 1, pp 316–326.

[15] Rehmani, MH., Reisslein, M., Rachedi, A., Erol-Kantarci, M., Radenkovic, M. Integrating renewable energy resources into the smart grid: Recent developments in information and communication technologies. IEEE Trans Ind Inf, 2018, 14, 7, pp 2814-2825.

[16] Mozafar, MR., Moradi, MH., Amini, MH. A simultaneous approach for optimal allocation of renewable energy sources and electric vehicle charging stations in smart grids based on improved GA-PSO algorithm. Sustain Cities Soc, 2017, 32, pp 627-637.

[17] Telukunta, V., Pradhan, J., Agrawal, A., Singh, M., Srivani, SG. Protection challenges under bulk penetration of renewable energy resources in power systems: a review. CSEE J Power Energy Syst. 2017, 3, 4, pp 365-379.

[18] Khojasteh, D., Khojasteh, D., Kamali, R., Beyene, A., Iglesias, G. Assessment of renewable energy resources in Iran; with a focus on wave and tidal energy. Renew Sustain Energy Rev, 2017, 81, 2, pp 2992-3005.

[19] Liu, G., Li, M., Zhou, B., Chen, Y., Liao, S. General indicator for techno-economic assessment of renewable energy resources. Energy Convers Manage, 2018, 156, pp 416–426.

[20] Nematollahi, O., Hoghooghi, H., Rasti, M., Sedaghat, A. Energy demands and renewable energy resources in the Middle East. Renew Sustain Energy Rev, 2016, 54, pp 1172–1181.

[21] Van der Zwaan, B., Cameron, L., Kober, T. Potential for renewable energy jobs in the Middle East. Energy Policy, 2013, 60, pp 296–304.

[22] Mostafaeipour, A., Mostafaeipour, N. Renewable energy issues and electricity production in Middle East compared with Iran. Renew Sustain Energy Rev, 2009, 13, pp 1641–1645.

[23] Rourke, FO., Boyle, F., Reynolds, A. Renewable energy resources and technologies applicable to Ireland. Renew Sustain Energy Rev, 2009, 13, pp 1975–1984.

[24] Global tracking framework, www.worldbank.org/se4all, accessedon24/6/2013.

[25] Amini, MH., Moghaddam, MP., Karabasoglu, O. Simultaneous allocation of electric vehicles' parking lots and distributed renewable resources in smart power distribution networks. Sustain Cities Soc, 2017, 28, pp 332-342.

[26] Wang, Y., Xu, L., Solangi, YA., Strategic renewable energy resources selection for Pakistan: Based on SWOT-Fuzzy AHP approach. Sustain Cities Soc, 2020, 52, doi: https://doi.org/10.1016/j.scs.2019.101861.

[27] Amini, MH., Nabi, B., Haghifam, M. Load management using multi-agent systems in smart distribution network. Power and Energy Society General Meeting (PES), Vancouver, BC, Canada, 21-25 July 2013.

[28] de Lucena AFP, Szklo AS, Schaeffer R, Dutra RM. The vulnerability of wind power to climate change in Brazil. Renew Energy, 2010, 35, pp. 904–912.

[29] Viviescas, C., Lima, L., Diuana, FA., Vasquez, E., Ludovique, C., Silva, GN., Huback, V., Magalar, L., Szklo, A., Lucena, AFP., Schaeffer, R., Paredes, JR., Contribution of Variable Renewable Energy to increase energy security in Latin America: Complementarity and climate change impacts on wind and solar resources. Renew Sustain Energy Rev, 2019, 113, https://doi.org/10.1016/j.rser.2019.06.039.

[30] Arasteh, H., Sepasian, MS., Vahidinasab, V., Siano, P. SoS-based multiobjective distribution system expansion planning. Electr Power Syst Res, 2016, 141, pp 392–406.

[31] Vilaça Gomes, P. Saraiva, JT. A novel efficient method for multiyear multiobjective dynamic transmission system planning. Int J Electr Power Energy Syst, 2018, 100, pp 10-18.

[32] Mavalizadeh, H. Ahmadi, A. Hybrid expansion planning considering security and emission by augmented epsilon-constraint method. Int J Electr Power Energy Syst, 2014, 61, pp 90-100.

[33] V. Vahidinasab. Optimal distributed energy resources planning in a competitive electricity market: Multiobjective optimization and probabilistic design. Renew. Energy, 2014, 66, pp 354-363.

[34] Ellaia, R., El Mouatasim, A., Banga, J. R., Sendin, O. H., NBI-RPRGM for multi-objective optimization design of bio-processes. ESAIM: Proc, 2007, 20, pp. 118–128.

[35] Monsef, H., Naghashzadegan, M., Jamali, A., Farmani, R., Comparison of evolutionary multi objective optimization algorithms in optimum design of water distribution network. Ain Shams Eng J, 2019, 10, 1, pp. 103-111.

[36] Costa, DMD., Brito, TG., de Paiva, AP., Leme, RC., Balestrassi, PP., A normal boundary intersection with multivariate mean square error approach for dry end milling process optimization of the AISI 1045 steel. J Clea Prod, 2016, 135, pp. 1658-1672.

[37] Ahmadi, A., Moghimi, H., Nezhad, A.E., Agelidis, VG., Sharaf, A.M., Multi-objective economic emission dispatch considering combinedheat and power by normal boundary intersection method. Electr Power Syst Res. 2015, 129, pp. 32–43.

[38] Ganesan, T., Elamvazuthi, I., Vasant, P., Evolutionary Normal-Boundary Intersection (ENBI) method for multi-objective optimization of green sand mould system. IEEE Int Conf Control Syst, Comput Eng., 25-27 Nov. 2011, pp. 86-91.

[39] Stehr, G, Graeb, HE., Antreich, KJ., Analog performance space exploration by normal-boundary intersection and by fourier–motzkin elimination. IEEE Trans Comput Aided Des Integr Circuits Syst, 2007, 26, 10, pp. 1733-1748.

[40] Shukla, A., Singh, SN., Multi-objective unit commitment using search space-based crazy particle swarm optimisation and normal boundary intersection technique. IET Gener Transm Distrib, 2016, 10, 5, pp. 1222–1231.

[41] Messac, A., Ismail-Yahaya, A., Mattson, CA. The normalized normal constraint method for generating the Pareto frontier. Struct Multidiscip O, 2003, 25, pp 86–98.

[42] Rahmani, S., Amjady, N. Improved normalised normal constraint method to solve multi-objective optimal power flow problem. IET Gener Transm Distrib, 2018, 12, 4, pp 859-872.

[43] Messac, A., Mattson, CA. Normal constraint method with guarantee of even representation of complete pareto frontier. AIAA J., 2004, 42, pp. 2101–2111.

[44] Zakariazadeh, A., Jadid, S., Siano, P. Stochastic multi-objective operational planning of smart distribution systems considering demand response programs. Electr Power Syst Res, 2014, 111, pp 156–168.

[45] Dhillon, JS., Parti, SC., Kothari, DP., Fuzzy decision making in multiobjective long-term scheduling of hydrothermal system. Int J Electr Power Energy Syst, 2001, 23, 1, pp. 19-29.

[46] Momoh JA, Ma XW, Tomsovic K. Overview and literature survey of fuzzy set theory in power systems. IEEE Trans Power Syst, 1995, 10, 3, pp. 1676–90.

[47] Tapia CG, Murtagh BA. Interactive fuzzy programming with preference criteria in multiobjective decision making. Comput Oper Res, 1991, 18, 3, pp. 307–16.

[48] Zhang, H., Vittal, V., Heydt, GT., Quintero, J. A mixed-integer linear programming approach for multi-stage security-constrained transmission expansion planning. IEEE Trans Power Syst, 2012, 27, 2, pp 1125–1133.

[49] MacQueen, J. Some methods for classification and analysis of multivariate observations. Proceedings of the Fifth Berkeley Symposium on Mathematical Statistics and Probability, 1967, 1, pp 281–297.

[50] National Renewable Energy Laboratory. System advisor model (SAM), https://sam.nrel.gov/content/downloads, 2015.

[51] Vahidinasab, V., Jadid, S., Joint economic and emission dispatch in energy markets: A multiobjective mathematical programming approach. Energy, 2010, 35, pp 1497–1504.

[52] Vahidinasab V, Jadid S. Multiobjective environmental/techno-economic approach for strategic bidding in energy markets. Applied Energy. 2009 Apr 1;86(4):496-504.

[53] Villasana, R., Garver, L., Salon, S. Transmission network planning using linear programming, IEEE Trans. Power Appar. Syst, 1985, PAS-104, 2, pp. 349–356.